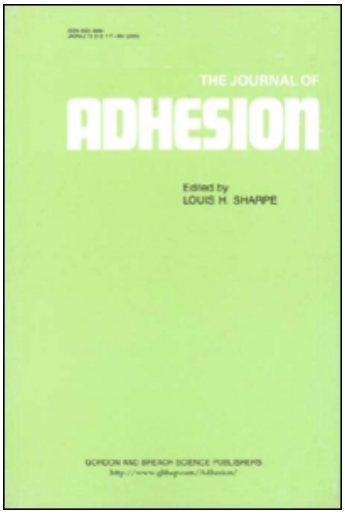

The Journal of Adhesion
Publication details, including instructions for authors and subscription information:
http://www.informaworld.com/smpp/title~content=t713453635

Two-Dimensional Thermal Stress Analysis in Adhesive Butt Joints Containing Hole Defects and Rigid Fillers in Adhesive Under Non-Uniform Temperature Field

Yuichi Nakano[a]; Masahide Katsuo[a]; Masataka Kawawaki[a]; Toshiyuki Sawa[b]
[a] Department of Mechanical Engineering, Shonan Institute of Technology, Tsujido, Fujisawa, Japan [b] Department of Mechanical Engineering, Yamanashi University, Kofu, Japan

To cite this Article Nakano, Yuichi , Katsuo, Masahide , Kawawaki, Masataka and Sawa, Toshiyuki(1998) 'Two-Dimensional Thermal Stress Analysis in Adhesive Butt Joints Containing Hole Defects and Rigid Fillers in Adhesive Under Non-Uniform Temperature Field', The Journal of Adhesion, 65: 1, 57 — 80
To link to this Article: DOI: 10.1080/00218469808012238
URL: http://dx.doi.org/10.1080/00218469808012238

J. Adhesion, 1998, Vol. 65, pp. 57–80
Reprints available directly from the publisher
Photocopying permitted by license only

Two-Dimensional Thermal Stress Analysis in Adhesive Butt Joints Containing Hole Defects and Rigid Fillers in Adhesive Under Non-Uniform Temperature Field

YUICHI NAKANO[a], MASAHIDE KATSUO[a], MASATAKA KAWAWAKI[a] and TOSHIYUKI SAWA[b]

[a]*Department of Mechanical Engineering, Shonan Institute of Technology, 1-1-25 Nishikaigan, Tsujido, Fujisawa 251, Japan;*
[b]*Department of Mechanical Engineering, Yamanashi University, 4-3-11 Takeda, Kofu 400, Japan*

(Received 23 September 1996; In final form 21 February 1997)

This study is concerned with the thermal stress analysis of an adhesive butt joint which contains circular holes and rigid fillers in an adhesive and is under a non-uniform temperature field. In the analysis, the adherends are assumed to be rigid and the adhesive is replaced with a finite strip having holes and rigid fillers in it and the thermal stress distribution in the adhesive is analyzed using a two-dimensional theory of elasticity. The effects of size and location of the circular holes and rigid fillers on the stress distributions at the interface and at the hole and filler peripheries are clarified by numerical calculations. For verification, photoelastic experiments were performed using an epoxide resin plate with small holes and fillers in it, to model and adhesive in the joint. The analytical results are fairly consistent with the experimental ones.

Keywords: Elasticity; thermal stress analysis; adhesive butt joint; hole defect; rigid filler; photoelasticity; thermoelastic potential

1. INTRODUCTION

Adhesive joints are now widely used in mechanical structures because of easy joining of different materials, lightened joined structure, uniform stress distribution and so on. However, a lot of difficulties still

remain and should be overcome in order to apply adhesive joints at important parts of machine structures with sufficient reliability. The thermal strength of the adhesive joint is one of the main problems since the mechanical and thermal properties of an adherend and an adhesive are generally quite different so that thermal stresses are generated easily in the joint [1–4]. In practical joints, and adhesive often contains fillers of various kinds of materials or small air holes created in applying it on the surfaces to be bonded. Recently, some experimental work [5–7] has been carried out on the improvement of static and dynamic strengths of adhesively-bonded joints by adding fillers such as rubber, alumina, and metal particles into an adhesive. However, analytical studies concerning the thermal strength of adhesive joints which contain such kinds of fillers and hole defects in an adhesive are few and adhesives are mostly assumed to contain no such hole defects or fillers.

The authors have investigated analytically and experimentally the effects of the holes and/or fillers on the stress distribution in adhesive joints subjected to a tensile load [8, 9], a bending load [10] and a thermal load [11, 12]. From these investigations, it is clarified that when the joints have holes or fillers in the adhesive, the stress concentration occurs at the hole or filler periphery and its magnitude varies with the hole or filler size and location. Moreover, the stress concentration affects the stress distribution at the interface between the adherends and the adhesive which often becomes singular at the edge of the interface. Both the stress concentration at the hole or filler periphery and the stress singularity at the edge of the interface have an important role in the joint strength. Therefore, for practical use of adhesive joints, it is necessary to examine the effects of hole defects and fillers in an adhesive on the mechanical and thermal characteristics of the adhesive joints.

The purpose of this study is to clarify the effects of both circular holes and rigid fillers contained in an adhesive on the thermal stress distribution in adhesive butt joints where the adherends are under different constant temperatures. In the analysis, the adherends are replaced with semi-infinite strips and the adhesive is modelled as a finite strip with circular holes and rigid fillers. First, the steady state temperature distribution in the adhesive is calculated analytically and then the thermal stress distribution is analyzed using a two-dimensional theory of elasticity and an iteration method. The effects of size

and location of circular holes and rigid fillers on the thermal stress distributions at the interface between the adherend and the adhesive and at the hole and filler peripheries have been clarified by numerical calculations. In addition, the analytical results have been compared with the photoelastic experimental results.

2. THEORETICAL ANALYSIS

Figure 1 shows an analytical model of an adhesive butt joint in which two similar adherends are joined by an adhesive containing two circular holes of radius a at $\pm x_0$ on the x axis symmetrically with respect to the y axis and a filler of the same radius a at the center of an adhesive. The upper and lower adherends are kept at constant temperatures T_1 and T_2, respectively, and heat transfer occurs between the side surfaces of the joint and the ambient air at 0°C with a heat transfer coefficient α.

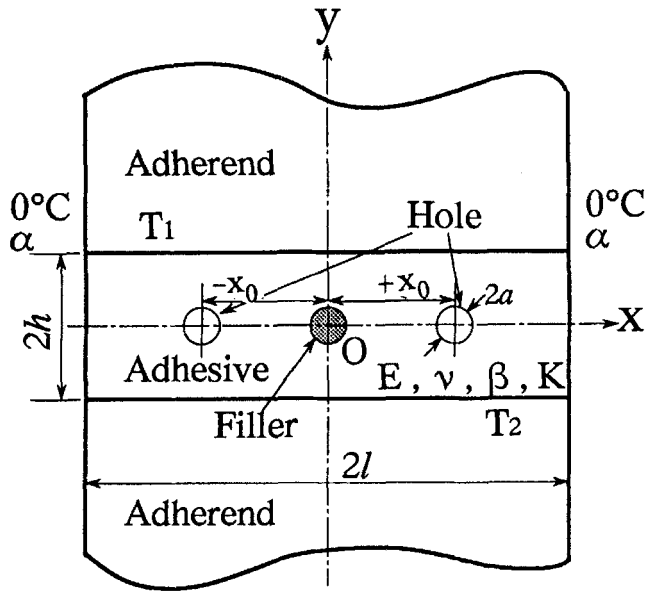

FIGURE 1 Model for analysis of adhesive butt joint containing circular holes and a rigid filler in an adhesive.

In the analysis, the adhesive is replaced with a finite strip, the height and width of which are denoted as $2h$ and $2l$, and the Young's modulus, Poisson's ratio, coefficient of thermal expansion and thermal conductivity are E, ν, β and K, respectively. The following assumptions are made in this analysis: (1) The material properties are constant and independent of temperature; (2) There is no temperature distribution in the z-direction of the joint, *i.e.*, we have a two-dimensional heat transfer problem; (3) The adherends and fillers are rigid; (4) No external load acts on the joint.

2.1. Temperature Distribution

At first, the temperature distribution $T(x, y)$ in an adhesive containing no holes and fillers is analyzed. In the case of the steady state, the temperature distribution is expressed as Eq. (1) and the thermal boundary conditions of the joint are given by Eq. (2).

$$\nabla^2 T(x, y) = 0 \tag{1}$$

$$T(x, +h) = T_1, \quad T(x, -h) = T_2, \quad -K\frac{\partial T(\pm l, y)}{\partial x} = \alpha T(\pm l, y) \tag{2}$$

In order to simplify the analysis of temperature distribution, the effects of holes and fillers in the adhesive on the temperature distribution are neglected. Thus, Eq. (1) can be simply solved and expressed as Eq. (3) by using a separation of variables method under the thermal conditions of Eq. (2).

$$T(x, y) = \sum_{i=1}^{\infty} \{A_i \cosh(k_i y) + B_i \sinh(k_i y)\} \cos(k_i x) \tag{3}$$

where

$$A_i = \frac{2(T_1 + T_2)\sin(k_i l)}{\cosh(k_i h)\{\sin(2k_i l) + 2k_i l\}}, \quad B_i = \frac{2(T_1 - T_2)\sin(k_i l)}{\sinh(k_i h)\{\sin(2k_i l) + 2k_i l\}}$$

and, k_i is the i-th positive root satisfying $k_i \tan(k_i l) = \alpha/K$.

However, if the ratio of a heat conductivity of the filler to that of the adhesive is extremely large, it is necessary to analyze the temperature distribution taking the effect of the filler into consideration [12]. The effect of the hole on the temperature distribution is generally smaller as compared with that of the filler.

2.2. Thermal Stress

The boundary conditions of the joint concerning the stresses and the displacements are expressed as Eq. (4.a) at the free side surfaces of the adhesive ($x = \pm l$) and at the interface between the adherend and the adhesive ($y = \pm h$), as Eq. (4.b) at hole peripheries and as Eq. (4.c) at filler peripheries in the adhesive.

$$\sigma_x = \tau_{xy} = 0 \quad (x = \pm l), \quad u_x = \frac{\partial v_y}{\partial x} = 0 \quad (y = \pm h) \tag{4.a}$$

$$\sigma_r = \tau_{r\theta} = 0 \quad (r = a) \tag{4.b}$$

$$u_r = v_\theta \quad (r = a) \tag{4.c}$$

where u_x and v_y denote the displacements in the x and y directions, respectively, and u_r and v_θ the displacements in the r and θ directions in polar coordinates, respectively.

In this study, a thermoelastic potential approach is adopted for the thermal stress analysis. Generally, the thermoelastic potential $\Omega(x, y)$ is expressed by the temperature distribution $T(x, y)$ and Eq. (5) and the thermal stresses σ_x, σ_y, τ_{xy} and the displacements u_x and v_y obtained from $\Omega(x, y)$ are expressed as Eq. (6).

$$\nabla^2 \Omega(x, y) = T(x, y) \tag{5}$$

$$\sigma_x = -E\beta \frac{\partial^2 \Omega(x, y)}{\partial y^2}, \quad \sigma_y = -E\beta \frac{\partial^2 \Omega(x, y)}{\partial x^2}, \quad \tau_{xy} = E\beta \frac{\partial^2 \Omega(x, y)}{\partial x \partial y},$$

$$2Gu_x = E\beta \frac{\partial \Omega(x, y)}{\partial x}, \quad 2Gv_y = E\beta \frac{\partial \Omega(x, y)}{\partial y} \tag{6}$$

where G is the shear modulus. From Eqs. (3) and (5), the thermoelastic potential $\Omega(x, y)$ for the adhesive is expressed as Eq. (7) and the thermal stresses and the displacements can be calculated from Eq. (6).

$$\Omega(x, y) = \sum_{i=1}^{\infty} \frac{1}{2k_i} \{A_i y \sinh(k_i y) + B_i y \cosh(k_i y)\} \cos(k_i x) \tag{7}$$

However, in practice, the boundary conditions concerning the stresses and the displacements of the adhesive, which are expressed as Eqs. (4), are not always satisfied by only the thermoelastic potential $\Omega(x, y)$. In order to satisfy the boundary conditions, the following procedure is adopted in the present analysis [11, 12].

Step 1: *Analysis of a finite strip containing no circular holes and rigid fillers in it.*

In order to satisfy the boundary condition Eq. (4.a), an adhesive containing no circular holes and rigid fillers is modelled by a finite strip, the height and width of which are denoted as $2h$ and $2l$, respectively, and is analyzed using the Airy stress function $\chi(x, y)$ in rectangular coordinates in order to eliminate the stresses σ_x, τ_{xy} at the free side surfaces ($x = \pm l$) and the displacement u_x, the gradient of the displacement $\partial v_y/\partial x$ at the interfaces between the adherend and the adhesive ($y = \pm h$) which are obtained from the thermoelastic potential $\Omega(x, y)$. Then the stresses σ_r and $\tau_{r\theta}$ at each hole periphery ($r = a$) and the displacements u_r and v_θ at each filler periphery ($r = a$) are given analytically from the stress function $\chi(x, y)$, as shown in Figure 2(a).

Step 2: *Analysis of an infinite strip containing a circular hole and a rigid filler in it.*

In order to eliminate the stresses σ_r and $\tau_{r\theta}$ at each hole periphery generated in the *Step 1* and to satisfy the boundary condition Eq. (4.b), an infinite plate in which a circular hole is contained is analyzed using the Airy stress function $\psi(r, \theta)$ in polar coordinates

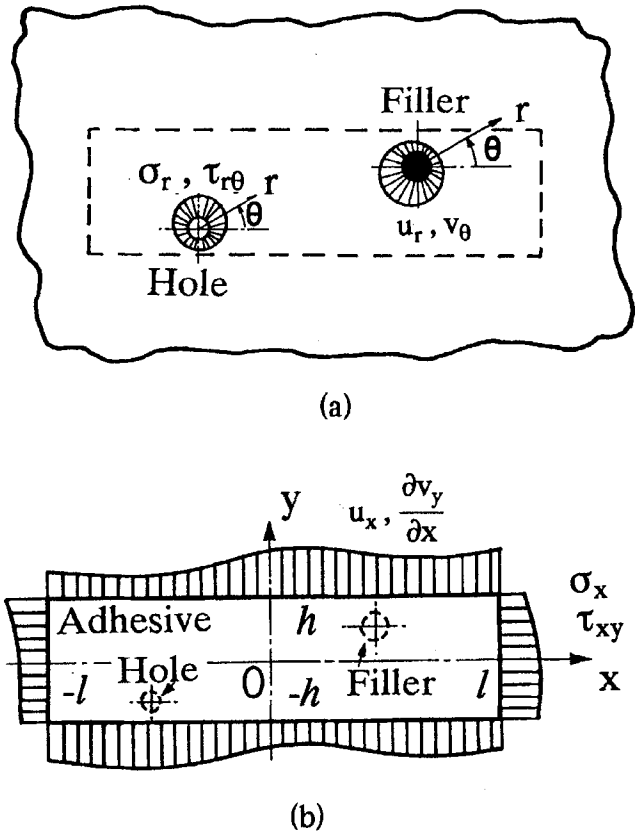

FIGURE 2 Illustration of analytical method, (a) Stresses at hole periphery and displacements at filler periphery, (b) Stresses and displacements at boundaries of adhesive.

which is expressed as Eq. (8).

$$\Psi(r,\theta) = A_0\theta + B_0 \log r + A_1 r \log r \cos\theta + B_1 r\theta \sin\theta$$
$$+ C_1 r\theta\cos\theta + D_1 r \log r \sin\theta$$
$$+ \sum_{n=2}^{\infty} (A_n r^{-n} + B_n r^{-n+2}) \cos n\theta$$
$$+ \sum_{n=2}^{\infty} (C_n r^{-n} + D_n r^{-n+2}) \sin n\theta \qquad (8)$$

where, A_0, B_0, A_n, B_n, C_n and D_n $(n = 1, 2, 3, \ldots)$ are unknown coefficients and can be determined by comparing the coefficients in the Fourier series of the negative stresses, $-\sigma_r$ and $-\tau_{r\theta}$, around each hole periphery. Similarly, an infinite plate in which a rigid filler is contained is analyzed using the similar stress function $\Psi(r, \theta)$ in order to eliminate the displacements u_r and v_θ around each filler periphery shown in Figure 2(a) and to satisfy the boundary condition of Eq. (4.c). The displacement u_x and the gradient of the displacement $\partial v_y/\partial x$ at the interfaces of the adhesive $(y = \pm h)$ and the stresses σ_x and τ_{xy} at the free side surfaces of the adhesive $(x = \pm l)$ are generated again analytically from this *Step 2*, as shown in Figure 2(b).

When the adhesive contains more than two holes or fillers, the displacement u_x and the gradient of the displacement $\partial v_y/\partial x$ at the interfaces and the stresses σ_x and τ_{xy} at the free side surfaces of the adhesive can be obtained by adding the stress and the displacement component from the stress function $\Psi(r, \theta)$ for each hole or filler periphery.

Step 3: *Analysis of a fintie strip with the displacement and the stress distributions at the boundaries.*

A finite strip is analyzed using the Airy stress function $\chi(x, y)$ which is expressed as Eq. (9) [3], in order to eliminate the displacement, the gradient of the displacement and the stresses generated in the *Step 2* at the interfaces and at the free side surfaces of the adhesive, respectively.

$$\chi(x, y) = \chi_0 + \chi_1 + \chi_2 + \chi_3 + \chi_4 \tag{9}$$

$$\chi_0 = \frac{A_0}{2} x^2 + \frac{B_0}{2} y^2 + \frac{C_0}{2} x^2 y$$

$$\chi_1 = \sum_{n=1}^{\infty} \frac{\bar{A}_n}{\bar{\Delta}_n \alpha_n^2} [\{\sinh(\alpha_n l) + \alpha_n l \cosh(\alpha_n l)\} \cosh(\alpha_n x)$$

$$- \sinh(\alpha_n l)\, \alpha_n x \sinh(\alpha_n x)] \cos(\alpha_n y)$$

$$+ \sum_{s=1}^{\infty} \frac{\bar{B}_s}{\bar{\Omega}_s \lambda_s^2} [\{\sinh(\lambda_s h) + \lambda_s h \cosh(\lambda_s h)\} \cosh(\lambda_s y)$$

$$- \sinh(\lambda_s h)\, \lambda_s y \sinh(\lambda_s y)] \cos(\lambda_s x)$$

$$\chi_2 = \sum_{n=1}^{\infty} \frac{\bar{\bar{A}}_n}{\bar{\bar{\Delta}}_n \alpha_n'^2} [\{\sinh(\alpha_n' l) + \alpha_n' l \cosh(\alpha_n' l)\} \cosh(\alpha_n' x)$$

$$- \sinh(\alpha_n' l)\, \alpha_n' x \sinh(\alpha_n' x)] \sinh(\alpha_n' y)$$

$$+ \sum_{s=1}^{\infty} \frac{\bar{\bar{B}}_s}{\bar{\bar{\Omega}}_s \lambda_s'^2} [\{\cosh(\lambda_s h) + \lambda_s h \sinh(\lambda_s h)\} \sinh(\lambda_s y)$$

$$- \cosh(\lambda_s h)\, \lambda_s y \cosh(\lambda_s y)] \cos(\lambda_s x)$$

$$\chi_3 = \sum_{n=1}^{\infty} \frac{\bar{A}_n'}{\bar{\Delta}_n' \alpha_n'^2} \{\cosh(\alpha_n' l)\, \alpha_n' x \sinh(\alpha_n' x)$$

$$- \alpha_n' l \sinh(\alpha_n' l) \cosh(\alpha_n' x)\} \cos(\alpha_n' y)$$

$$+ \sum_{s=1}^{\infty} \frac{\bar{B}_s'}{\bar{\Omega}_s' \lambda_s'^2} \{\cosh(\lambda_s' h)\, \lambda_s' y \sinh(\lambda_s' y)$$

$$- \lambda_s' h \sinh(\lambda_s' h) \cosh(\lambda_s' y)\} \cos(\lambda_s' x)$$

$$\chi_4 = \sum_{n=1}^{\infty} \frac{\bar{\bar{A}}_n'}{\bar{\bar{\Delta}}_n' \alpha_n^2} [\{\cosh(\alpha_n l)\, \alpha_n x \sinh(\alpha_n x)$$

$$- \alpha_n l \sinh(\alpha_n l) \cosh(\alpha_n x)\} \sin(\alpha_n y)$$

$$+ \sum_{s=1}^{\infty} \frac{\bar{\bar{B}}_s'}{\bar{\bar{\Omega}}_s' \lambda_s'^2} \{\sinh(\lambda_s' h)\, \lambda_s' y \cosh(\lambda_s' y)$$

$$- \lambda_s' h \cosh(\lambda_s' h) \sinh(\lambda_s' y)\} \cos(\lambda_s' x)$$

where

$$\alpha_n = \frac{n\pi}{h},\ \alpha_n' = \frac{(2n-1)\pi}{2h},\ \lambda_s = \frac{s\pi}{l},\ \lambda_s' = \frac{(2s-1)\pi}{2l}\ (n, s = 1, 2, 3, \ldots)$$

$A_0, B_0, C_0, \bar{A}_n, \bar{B}_s, \ldots, \bar{\bar{B}}_s'(n, s = 1, 2, 3, \ldots)$ in the equation are unknown coefficients and can be determined from the boundary condition of

Eq. (4.a). The displacements u_r and v_θ and the stresses σ_r and $\tau_{r\theta}$ are generated again at each rigid filler and circular hole periphery, respectively, from this solution.

The *Steps 2* and *3* are iterated until the boundary conditions of Eqs. (4) are satisfied sufficiently; finally, the thermal stress and the displacement distributions in the adhesive can be obtained.

3. EXPERIMENTAL METHOD

Figure 3 shows the dimensions of an adhesive butt joint used in the photoelastic experiment. An epoxide resin plate, the width, the height and the thickness of which were 80, 20 and 6 mm, respectively, was used as an adhesive and three holes of 5 mm diameter were drilled at the

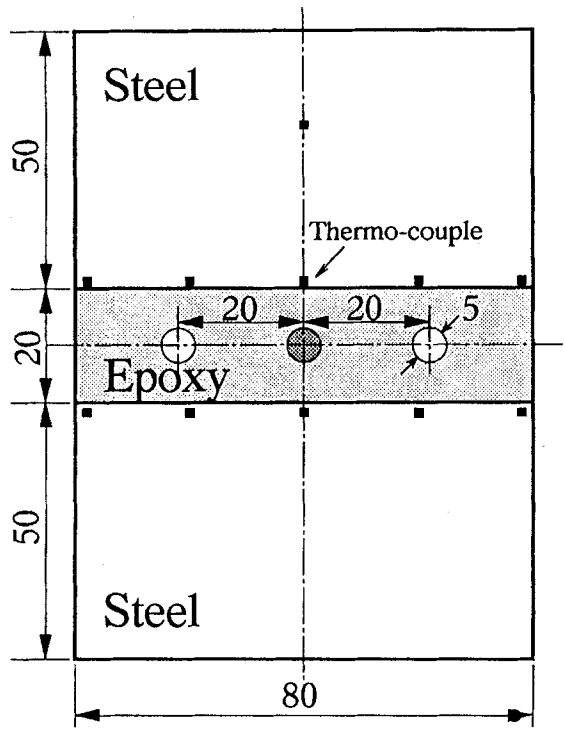

FIGURE 3 Dimensions of adhesive butt joint used in photoelastic experiment.

center and at ± 20 mm from the center of the plate by a water jet cutting machine to prevent residual stress generation during the manufacturing process. Structural steel (S25C, JIS) was used as the adherends and fillers and its Young's modulus (206GPa) was about 60 times as large as that of the epoxide resin plate (3.43GPa) so that the adherends and fillers were considered to be relatively rigid.

The bonding surfaces of the steel plates and the epoxide resin plate were finished by grinding and bonded together at a constant temperature by an epoxide adhesive (Sumitomo 3M, 1838B/A), the mechanical properties of which were similar to those of the epoxide resin plate. Simultaneously, in case of the joint shown in Figure 3, a filler was inserted into the center hole on the epoxide resin plate and bounded by the same adhesive. Afterwards, the two adherends were kept at different temperatures. The upper one was heated by thin electric heaters (50W/100V) attached on both front and back surfaces, and the lower one was cooled in temperature-controlled water as shown in Figure 4. The temperature distributions in each adherend were measured by thermocouples and, when the joint was at a steady state temperature, an isochromatic fringe pattern produced on the epoxide resin plate was observed by photoelasticity. It was confirmed in advane that internal stresses generated during the joint manufacturing

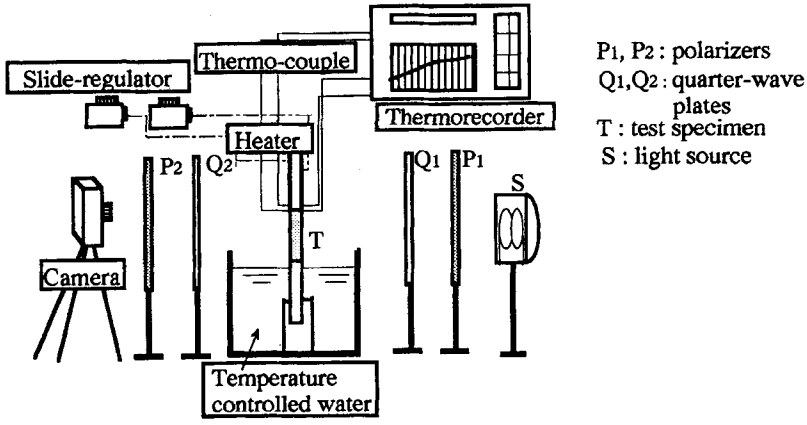

FIGURE 4 Experimental setup.

process were negligible over the entire epoxide plate from the observation of the isochromatic fringe pattern on the plate.

4. ANALYTICAL RESULTS

The effects of size and location of circular holes and rigid fillers in an adhesive on the thermal stress distributions at the interface between an adherend and an adhesive and at the hole and filler peripheries are examined numerically. In the numerical calculations, two kinds of adhesive butt joints are examined: (A) the joint where two circular holes are contained at $\pm x_0$, symmetrically with respect to the y axis and a rigid filler at the center of the adhesive, and (B) the joint where two rigid fillers and a circular hole are replaced *vice versa*. The truncated number, N, of terms of the series of infinite simultaneous equations which are derived from the stress functions $\chi(x, y)$ and $\Psi(r, \theta)$ is taken as 80 and the number of iterations is 5. The difference in the thermal stresses of the 5-th and 6-th iterations are within 1% in all calculations, so that satisfactory covergence is expected. A coefficient of heat transfer, α, between the free side surfaces of the adhesive and the ambient air of 0°C is taken as 20 W/m^2 K according to Reference [13].

4.1. Effects of Hole and Filler Size on the Thermal Stress Distributions

Various sizes of holes and fillers may be contained in the adhesive of real adhesive joints. Therefore the effects of the size of a hole and filler relative to the thickness of an adhesive on the stress distributions at the interface and at the hole and filler peripheries are examined. In the following calculations, it is assumed that the hole and filler size are the same, and both adherends are kept at lower temperatures than that of the ambient air of 0°C.

4.1.1. Joint (A) (Two Holes and a Filler)

Figure 5 shows the effects of a hole and filler radius to a half of the adhesive thickness, a/h, on the maximum principal thermal stress distributions: (a) at the interface between the adherend and the adhesive,

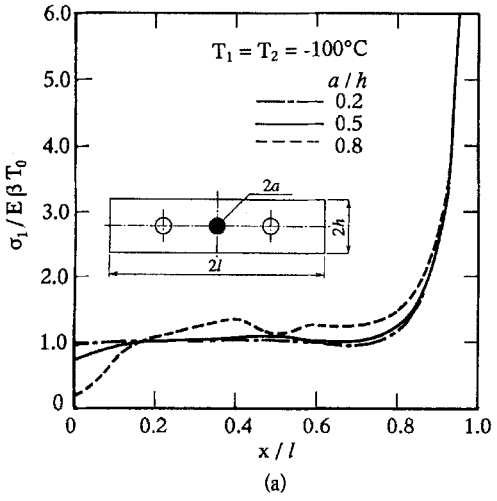

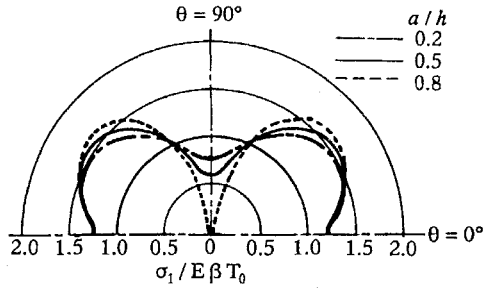

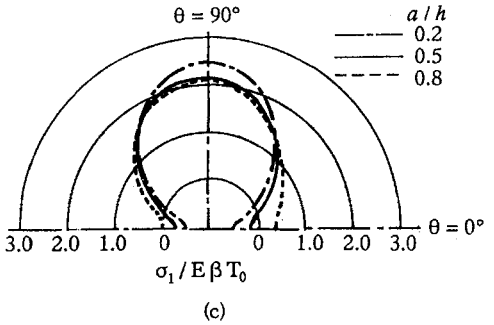

FIGURE 5 Effects of hole and filler size on maximum principal thermal stress distribution in joint (A) ($h/l = 0.2$, $x_0/l = 0.5$, $T_1 = T_2 = -100°C$), (a) At interface ($y = \pm h$), (b) At rigid filler periphery (center) (c) At circular hole periphery ($x_0 = 0.5l$).

(b) at a rigid filler periphery located at the center and (c) at a circular hole periphery located at $x_0 = 0.5l$ of the adhesive in joint (A) when the upper and the lower adherends are kept at the same temperature, $T_1 = T_2 = -100°C$. In the figures, the maximum principal thermal stress is normalized as $\sigma_1/E\beta T_0$, where T_0 denotes the absolute temperature difference between the adherend and the ambient air. The normalized maximum principal thermal stress distributions at a half interface in Figure 5(a) and at a half periphery ($0° < \theta < 180°$) in Figures 5(b) and (c) are shown because of the symmetry of the stress distribution.

From Figure 5(a), the normalized maximum principal thermal stress is tensile at the interface and is singular at the edge ($x/l = 1.0$). The thermal stress decreases with an increase of the radius, a, of the filler around the center of the interface where a rigid filler is contained beneath; however, in contrast, it becomes slightly larger with an increase of a hole radius, a, around the interface where a circular hole is contained beneath ($x_0 = 0.5l$). From Figure 5(b), the normalized maximum principal stress at the filler periphery increases with an increase of filler size and the maximum value occurs at the positions in the directions, θ, of $\pm 45°$ and $\pm 135°$. On the other hand, from Figure 5(c), the normalized maximum principal stress at the hole periphery increases with a decrease of hole size, and the maximum value occurs around positions in the thickness direction ($\pm 90°$) of the adhesive. By comparison between Figures 5(b) and (c), the normalized maximum principal stress at the hole periphery is larger than that at the filler periphery.

4.1.2. Joint (B) (A Hole and Two Fillers)

Figure 6 shows the effect of the ratio a/h on the normalized maximum principal thermal stress distributions: (a) at the interface between the adherend and the adhesive, (b) at a circular hole periphery located at the center and (c) at a rigid filler periphery located at $x_0 = 0.5l$ of the adhesive in joint (B). From Figure 6(a), the normalized maximum principal thermal stress decreases with an increase of filler size around the interface where a rigid filler is contained beneath ($x_0 = 0.5l$), similarly to joint (A) shown in Figure 5, and seems to be less sensitive to hole size around the center of the interface when the radius, a, is less

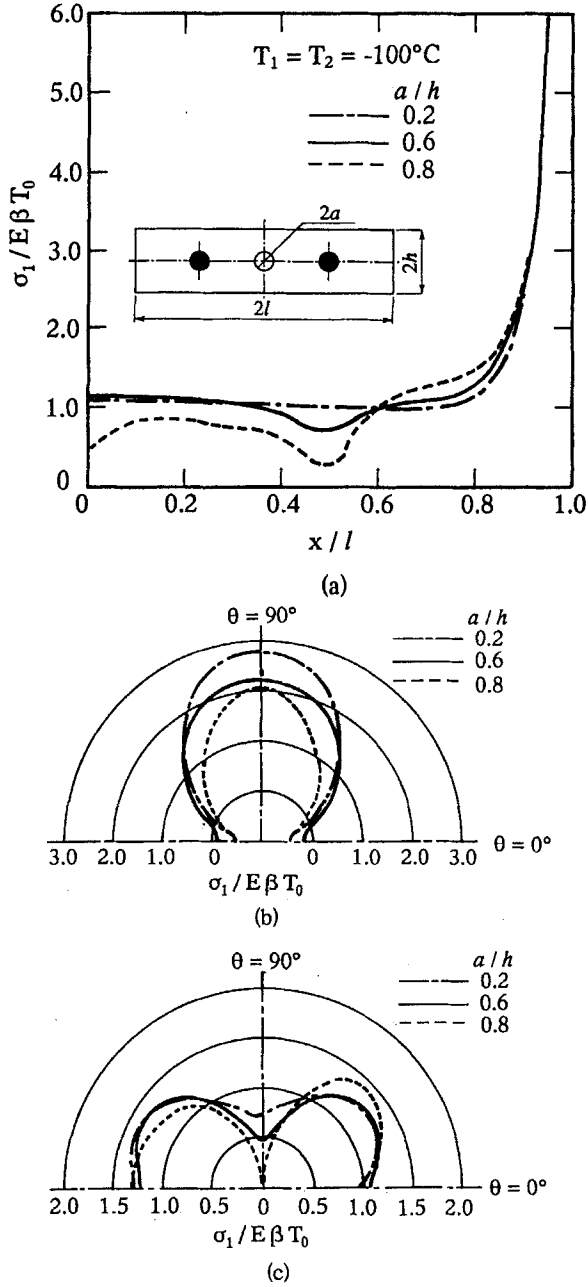

FIGURE 6 Effects of hole and filler size on maximum principal thermal stress distribution in joint (B) ($h/l = 0.2$, $x_0/l = 0.5$, $T_1 = T_2 = -100°C$), (a) At interface ($y = \pm h$), (b) At circular hole periphery (center) (c) At rigid filler periphery ($x_0 = 0.5l$).

than $0.6h$. However, it decreases steeply with an increase of hole radius as a becomes $0.8h$ or more. From Figure 6(b) and (c), it can be seen that the effects of filler and hole size on the normalized maximum principal stresses at each periphery are similar to joint (A). Thus, as the radius a increases, the maximum principal stress increases at the filler periphery and decreases at the hole periphery. From Figure 6(c), the stresses at the positions $\theta = \pm 45°$ can be seen to be larger than those at $\theta = \pm 135°$ of the filler as its radius increases. Also, the normalized maximum principal stress at the hole periphery is larger than that at the filler periphery, similar to joint (A).

From the results shown in Figures 5 and 6 the thermal stress is singular at the edge of the interface in both joints (A) and (B), and it is considered that the stress singularity may significantly affect the thermal strength of the joint [14, 15]. In the present calculating conditions, the maximum value of the principal stress near the edge of the interface is larger than that at the hole and filler peripheries. It is, therefore, predicted that the edge of the interface will be a fracture-initiating point under conditions of thermal stress. If and when the thermal fracture initiates in an adhesive, the hole periphery is likely to be the fracture-initiating point because its stress concentration is relatively larger than that at the filler periphery, especially in the case of small hole size.

4.2. Effects of Filler and Hole Location on the Thermal Stress Distribution

4.2.1. Thermal Stress Distribution at the Interface

Figure 7 shows the normalized maximum principal stress distribution at the interface in joint (B) when two fillers are contained near the free side surfaces of the adhesive ($x_0/l = \pm 0.7$, ± 0.8 and ± 0.9, $a = 0.2h$) in joint (B). The solid line in the figure is the case that the adhesive contains no holes and fillers. From the result, the thermal stress becomes smaller near the edge of the interface when rigid fillers are contained close to the free side surfaces of the adhesive than that in the joint with no holes and fillers in the adhesive. On the other hand, the effect of hole location on the thermal stress distribution at the interface in joint (A) is negligibly small in the present calculating conditions.

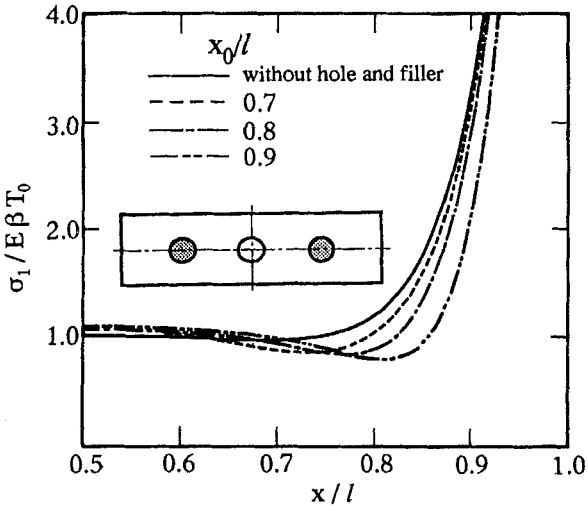

FIGURE 7 Effect of rigid filler position on maximum principal thermal stress distribution at interface in joint (B) ($h/l = 0.2$, $a/h = 0.2$, $T_1 = T_2 = -100°C$).

4.2.2. Thermal Stress Distributions at Hole and Filler peripheries

Figure 8 shows the normalized maximum principal stress distributions at the hole periphery in joint (A) when two holes of radius a of $0.2h$ are contained at $x_0 = \pm 0.3l$, $\pm 0.66l$ and $\pm 0.8l$. The stress becomes maximum in the thickness direction ($\theta = \pm 90°$) and increases slightly when holes are close to the center of the adhesive ($x_0 = \pm 0.3l$) and in the direction θ of $\pm 50° \sim 55°$ when holes are near the free side surfaces of the adhesive ($x_0 = \pm 0.8l$) and becomes minimum in the direction θ of 0° or 180° in all cases.

Figure 9 shows the maximum values of the normalized maximum principal stress at the hole and filler peripheries when the hole and filler positions, x_0, are varied in joints (A) and (B), respectively. From the results, the maximum principal stress at the hole periphery in joint (A), shown by a solid line in Figure 9, is larger than that at the filler periphery in joint (B), shown by a dotted line, except in the case that the hole, the radius of which is $0.2h$, is near the free side surface. In joint (B), the maximum principal stress at the filler periphery increases as the filler becomes close to the hole contained at the center of the

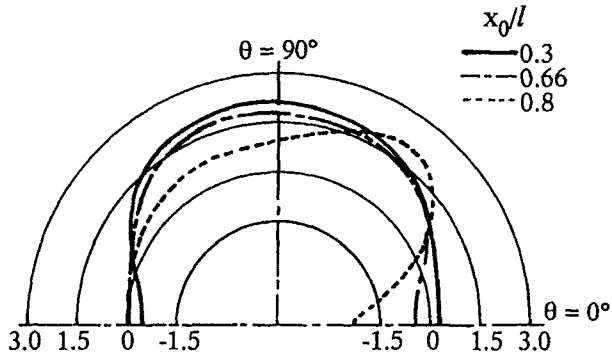

FIGURE 8 Effect of rigid filler position on maximum principal thermal stress distribution at periphery in joint (A) ($h/l = 0.2$, $a/h = 0.2$, $T_1 = T_2 = -100°C$).

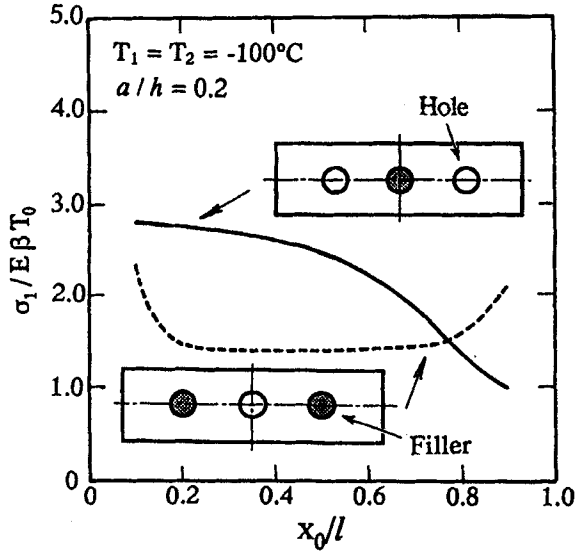

FIGURE 9 Effects of circular hole and rigid filler positions on maximum principal values at each periphery in joints (A) and (B) ($h/l = 0.2$, $a/h = 0.2$, $T_1 = T_2 = -100°C$).

adhesive or the free side surfaces of the adhesive and, in such joints, it is possible that the fracture may initiate at the filler periphery.

All the numerical results shown above are for the case where two adherends undergo the same temperature change from the bonding temperature, *i.e.*, $T_1 = T_2 = -100°C$.

4.3. The Case that Adherends are Kept at Different Temperatures

Figure 10 shows the maximum principal thermal stress distributions (a) at the upper and lower interface and (b) at the hole and filler peripheries in joint (A) where two adherends are kept at different temperatures, *i.e.*, the upper adherend is kept at $T_1 = -100°C$ and the lower one at $T_2 = 0°C$. A solid line in Figure 10 (a) indicates the stress at the interface between the lower temperature adherend ($-100°C$) and the adhesive, while a dotted line indicates the stress at the interface between the higher temperature adherend (0°C) and the adhesive. From the figure, the maximum principal thermal stress at the upper interface, where the temperature difference between the adherend and the ambient air is large, becomes larger than that at the lower interface.

The maximum principal stress at the filler periphery located at the center of the adhesive, shown by a solid line in Figure 10(b), is not affected by the temperature difference between the upper and the lower adherends. However, that at the hole periphery, shown by a dotted line, inclines with respect to the thickness direction so that the position of the maximum value of the stress differs from $\pm 90°$ in the joint where both the adherends are kept at the same temperature, as shown in Figure 5(c), to 55° and 235°.

5. EXPERIMENTAL RESULTS

Figure 11 shows examples of isochromatic fringe patterns generated on the epoxide resin plate modelled as an adhesive of joint (A). A rigid filler of 5 mm diameter is at the center and two holes of the same size are at ± 20 mm from the center of the plate. The numerical results of the principal stress difference which coincides with the isochromatic lines are also shown for a half (right hand) side of the epoxide plate. Numbers shown in numerical results indicate orders of the isochromatic lines. Figure 11(a) is the case where the upper and lower adherends are kept at the same temperature ($T_1 = T_2 = -20°C$) and Figure 11(b) is the case where these are at $T_1 = -15°C$ and $T_2 = -20°C$, respectively.

Similarly, the experimental and numerical results for joint (B), in which a hole is at the center and two fillers are at ± 20 mm from the center of the plate, are shown in Figure 12.

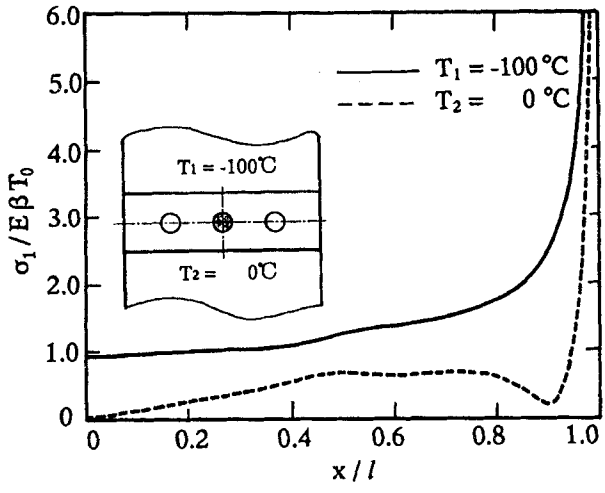

(a)

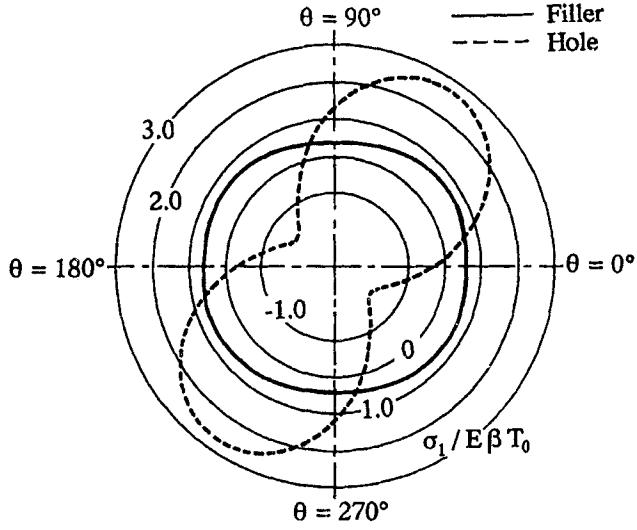

(b)

FIGURE 10 Effect of adherend temperature on maximum principal thermal stress distribution on joint (A) ($h/l = 0.2$, $a/h = 0.2$, $T_1 = -100°C$, $T_2 = 0°C$), (a) At interface ($y = \pm h$), (b) At circular hole and rigid filler peripheries.

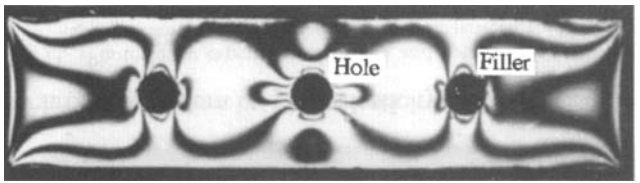

(a) Isochromatic pattern by photoelasticity (T_1=T_2=-20°C)

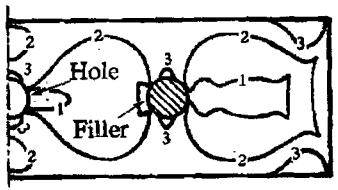

Numerically obtained isochromatic pattern

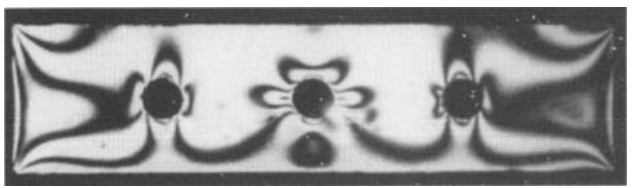

(b) Isochromatic pattern by photoelasticity (T_1=-15°C, T_2=-20°C)

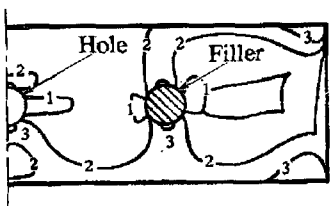

Numerically obtained isochromatic pattern

FIGURE 12 Photoelastic experimental results and comparison with numerical results in joint (B), (a) Isochromatic pattern by photoelasticity ($T_1 = T_2 = -20$°C). Numerically obtained isochromatic pattern, (b) Isochromatic pattern by photoelasticity ($T_1 = -15$°C, $T_2 = -20$°C). Numerically obtained isochromatic pattern.

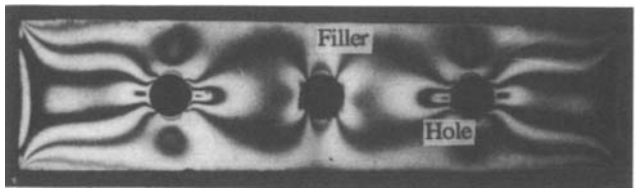

(a) Isochromatic pattern by photoelasticity (T_1=T_2=-20°C)

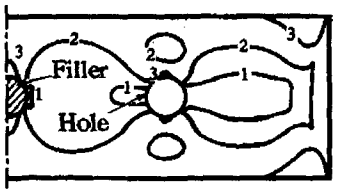

Numerically obtained isochromatic pattern

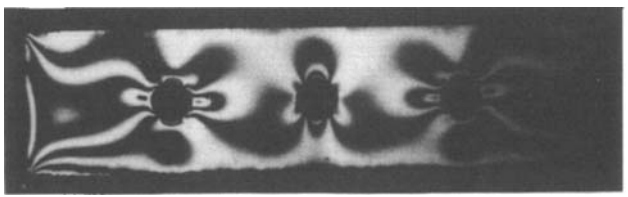

(b) Isochromatic pattern by photoelasticity (T_1=-15°C, T_2=-20°C)

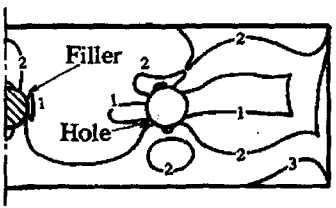

Numerically obtained isochromatic pattern

FIGURE 11 Photoelastic experimental results and comparison with numerical results in joint (A), (a) Isochromatic pattern by photoelasticity ($T_1 = T_2 = -20°C$). Numerically obtained isochromatic pattern, (b) Isochromatic pattern by photoelasticity ($T_1 = -15°C$, $T_2 = -20°C$). Numerically obtained isochromatic pattern.

From both Figures 11 and 12, the isochromatic lines obtained by photoelastic experiments are symmetrical with respect to the y axis of the joint and the thermal stress concentrates at the filler and hole peripheries and near the edges of the interfaces. Moreover, the numerical results are fairly consistent with the experimental results in each case.

6. CONCLUSIONS

This study deals with the thermal stress analysis in an adhesive butt joint which has circular holes and rigid fillers in the adhesive. The joint has a non-uniform temperature distribution, *i.e.*, the upper and lower adherends are kept at different temperatures and heat transfers between the side surfaces of the joint and the ambient air. The effects of size and location of a hole and a filler on the maximum principal thermal stress distributions at the interface between the adherend and the adhesive and at the hole and filler peripheries are clarified using numerical calculations. An epoxide resin plae was used to model the adhesive and the thermal stress distribution was measured by photoelastic experiment and compared with the analytical ones. The results obtained are as follows.

(1) An analytical method using a two-dimensional theory of elasticity has been used to analyze the steady-state thermal stress distribution in an adhesive butt joint where the adherends are kept at different temperatures from the bonding temperature and circular holes and rigid fillers are contained in the adhesive.
(2) The maximum principal stress is tensile at the interface between the adherend and the adhesive when the adherends are kept at a lower temperature than the bonding temperature.
(3) The maximum principal stress becomes singular at the edges of the interface and it decreases near the edges when rigid fillers are contained close to the free side surfaces of the adhesive.
(4) The stress concentration at the hole periphery is larger than that at the filler periphery, except for the case that fillers are contained close to the free side surfaces of the adhesive. Also, the stress concentration at the hole periphery increases with a decrease of the hole size.
(5) When the adherends are kept at different temperatures, the maximum principal stress becomes large at the interface where the temperature difference between the adherend and the ambient air is large.

(6) Photoelastic experiments were carried out in order to confirm the present thermal stress analysis and the experimental results were consistent with the numerical ones.

References

[1] Renton, W. J. and Vinson, J. R., "Analysis of Adhesively Bonded Joints between Panels of Composite Materials", *J. Appl. Mechanics* **44**, 101–106 (1977).
[2] Chen, D. and Cheng, S., "Stress Distribution in Plane Scarf and Butt Joints", *J. Appl. Mechanics* **57**, 78 (1990).
[3] Nakano, Y., Sawa, T. and Nakagawa, F., "Two-Dimensional Thermal Stress Analysis of Butt Adhesive Joints", *JSME Int. J.* **35**, 145–151 (1992).
[4] Adams, R. D. and Mallick, V., "The Effect of Temperature on the Strength of Adhesively-Bonded Composite-Aluminium Joints", *J. Adhesion* **43**, 17–33 (1993).
[5] Sohn, J. E., "Improved Matrix-Filler Adhesion", *J. Adhesion* **19**, 15–27 (1985).
[6] Young, R. J., in *Structural Adhesives*, Kinloch, A. J., Ed. (Elsevier Applied Science, London and New York, 1986), Chap. 6.
[7] Jakusik, R., Jamarani, F. and Kinloch, A. J., "The Fracture Behavior of a Rubber-Modified Epoxy Under Impact Fatigue," *J. Adhesion* **32**, 245–254 (1990).
[8] Nakano, Y., Temma, K. and Sawa, R., "A Two-dimensional Stress Analysis of Butt Adhesive Joints Having a Circular Hole in Adhesive", *JSME Int. J.* **31**, 507–513 (1988).
[9] Sawa, T., Nakano, K. and Nakano, Y., "A Two-dimensional Stress Analysis of a Butt Adhesive Joint Containing Circular Holes and Rigid Fillers in an Adhesive Subjected to a Tensile Load", *Proc. ASME/JSME Pressure Vessels & Piping Conf.* **302**, 119–119 (1995).
[10] Temma, K., Sawa, T., Uchida, H. and Nakano, Y., "A Two-Dimensional Stress Analysis of Butt Adhesive Joints Having a Circular Hole Defect in the Adhesive Subjected to External Bending Moments", *J. Adhesion* **33**, 133–147 (1991).
[11] Nakagawa, F., Sawa, T., Nakano, Y. and Hagiwara, S., "A Thermal Stress Analysis of Soldered/Bonded Joints with Defects", *Proc. ASME International Electronics Packaging Conference*, Engel, P. A. and Chen, W. T., Eds., **1**, 49–54 (1993).
[12] Nakagawa, F., Nakano, Y. and Sawa, T., "Two-Dimensional Thermal Stress Analysis of Butt Adhesive Joint Having Rigid Fillers in the Adhesive", *JSME Int. J.* **37**, 238–245 (1994).
[13] Thomas, L. C., *Heat Transfer* (Prentice Hall, New Jersey, 1993), p. 18.
[14] Bogy, D. B., "Two Edge-Bonded Elastic Wedges of Different Materials and Wedge Angles Under Surface Tractions", *J. Appl. Mechanics* **38**, 377–386 (1971).
[15] Hattori, T., "A Stress-Singularity-Parameter Approach for Evaluating the Adhesive Strength of Single-Lap Joints", *JSME Int. J.* **34**, 326–331 (1991).